Flight Demonstration of Non-Cooperative Rendezvous using Optical Navigation

S. D'Amico[1], J.-S. Ardaens[1], G. Gaias[1], B. Schlepp[1], H. Benninghoff[1], T. Tzschichholz[1], T. Karlsson[2], J. L. Jørgensen [3]

[1]*DLR, Oberpfaffenhofen, 82234 Wessling, Germany, +498153282115, simone.damico@dlr.de*
[2]*OHB Sweden, Solna Strandvaeg 86, 17122 Solna, Sweden, thomas.karlsson@ohb-sweden.se*
[3]*DTU Space, Elektrovej, Building 327, DK-2800 Lyngby, Denmark, jlj@space.dtu.dk*

Abstract: *The ultimate goal of this work is to demonstrate the capability of a maneuverable servicer spacecraft to rendezvous with a non-cooperative space resident object from far-range distance using optical angles-only measurements. To this end, the Advanced Rendezvous experiment using GPS and Optical Navigation (ARGON) has been executed during the extended phase of the PRISMA formation-flying mission in April 2012. This paper addresses the experiment design, the developed flight dynamics system, the obtained flight results, and the lessons learned. Furthermore the evaluation of the rendezvous tracking, navigation and control accuracy is performed by means of GPS-based precise relative orbit determination products. The presented results give a clear demonstration of the high readiness level reached by key technologies which are needed by future on-orbit servicing and debris-removal missions.*

Keywords: *flight results, vision-based navigation, angles-only tracking, rendezvous, PRISMA.*

1. Introduction

This work is mainly motivated by the new generation of on-orbit-servicing and debris-removal missions which are under considerations by several national and international space agencies [1,2]. These projects are driving the demand to efficiently approach and rendezvous with non-cooperative on-orbit objects. Strategic applications of this technology are in the frame of space situational awareness, orbital lifetime prolongation, and science among others. Common to these missions is the necessity to approach a non-cooperative passive target from large distances (e.g., > 30 km) in a fuel efficient, safe, and accurate manner. This poses new challenges as compared to the most recent in-orbit demonstrations [3,4]. Here, the usage of cooperative relative GPS techniques is mandatory to estimate and autonomously control the relative motion between the co-orbiting spacecraft. Measurements techniques alternative to GPS have been used in the past for rendezvous navigation such as radar or lidar instruments [5]. These sensors can provide relative range and angle measurements to the target, but at high cost in terms of power and weight requirements for the servicer spacecraft design.

On the contrary, many simple passive low cost sensors can provide line-of-sight direction, such as optical or infrared cameras. As a matter of fact, nowadays any spacecraft is equipped with star trackers which, if properly oriented, can be used to track where a space object is located within the field-of-view. Indeed this typology of sensor is considered as a very attractive solution to perform relative navigation tasks based on angles-only measurements [6]. The potential of angles-only navigation for orbital rendezvous has been recognized by various authors in the past [7—9], although, to the authors knowledge, the only published in-orbit demonstrations of angles-only navigation for autonomous rendezvous have been conducted in the frame of the Swedish PRISMA mission [10].

This work expands on the previous literature and demonstrates ground-based, far-range rendezvous to a non-cooperative and unknown client using angles-only navigation in the frame of a flight experiment conducted in April 23-27, 2012 during PRISMA [10]. In contrast to previous flight demonstrations, here an attempt has been made to generalize the rendezvous strategy and improve the portability and applicability of the developed techniques to other missions. The primary instrument used for angles-only navigation is the Vision-Based Sensor (VBS) of the Danish Technical University (DTU) embarked on the active Mango spacecraft [7]. This is used for vision-based navigation of Mango with respect to the passive Tango, which act respectively as servicer and client vehicles during the experiment. One of the four available VBS camera heads is used for far-range navigation through the collection of images. These are stored on-board, later down-linked during ground-contacts, and finally processed on-ground to extract line-of-sight information for relative navigation. In order to mimic a lost-in-space situation, no a-priori knowledge of the target vehicle is used during the experiment apart from Two-Line-Elements (TLEs) delivered by the North American Aerospace Defense Command (NORAD). Precise relative orbit determination products based on carrier-phase differential GPS [4] were only used post-facto, after the conclusion of the experiment, to assess the accuracy of the tracking, navigation, and control tasks.

In order to fulfill the experiment objectives, a flight dynamics system has been specifically developed which is characterized by numerous novelties as compared to the existent literature. The parameterization of the relative motion is based on the relative eccentricity and inclination vectors [11], which are used for the first time to enhance angles-only navigation and exploit the system properties of partial observability. This approach decouples the state components to a large extent and allows a straightforward separation of observable and unobservable parameters. Since the non-observability of the system is mainly condensed in the relative mean argument of latitude, the shape of the relative motion can be determined from the early phases of the approach based on the observable relative orbital elements [12]. This early knowledge of the geometry allows performing safe approaches by setting a proper relative eccentricity and inclination vector separation [11]. At the same time, the estimation error of the relative mean argument of latitude can be decreased through the execution of a dedicated maneuvers' profile as described in the paper. An iterative batch least squares filtering scheme has been adopted in this paper for relative orbit determination. This is the most reliable strategy in the context of a ground-based operational scenario characterized by large data gaps, possible outliers and unknown offsets in the acquired angle measurements. Throughout the experiment, orbit control maneuvers are planned on-ground and executed regularly by the servicer to track a pre-defined guidance profile. The guidance profile is specifically designed to realize the desired rendezvous while ensuring system observability, safety, fuel efficiency, and the presence of the client in the field of view (i.e., visibility).

This introduction is followed by an overview of the PRISMA mission and spacecraft. The so-called Advanced Rendezvous demonstration using GPS and Optical Navigation (ARGON) is described in the third section. The fourth section focuses on the developed flight dynamics system and its key software modules. The fifth section presents the flight results obtained during ARGON, including image processing, and performance assessment of the relative navigation and control tasks. The sixth and final section is dedicated to the lessons learned, way forward, and the potential applications of this novel technology to current and future strategically relevant missions.

2. Flight Configuration

The Prototype Research Instruments and Space Mission technology Advancement (PRISMA) consists of two spacecraft, namely Mango and Tango (see Fig. 1). In the following, the spacecraft are often referred to as servicer and client due the respective roles played during the ARGON experiment. The Mango spacecraft is 3-axis stabilized via star trackers and reaction wheels and is equipped with a propulsion system providing full 3D orbit control capability independent from the attitude. Tango is also 3-axis stabilized through a solar-magnetic control system, but does not have any orbit control capability. On June 15, 2010, the two spacecraft were launched clamped together into a 720/780 km altitude dawn-dusk sun-synchronous orbit. After an initial period of commissioning, Tango was separated and successfully acquired on August 11, 2010. The mission includes the flight qualification of several sensor and actuator systems as well as the in-flight execution of a range of guidance, navigation, and control (GNC) experiments using this equipment [10].

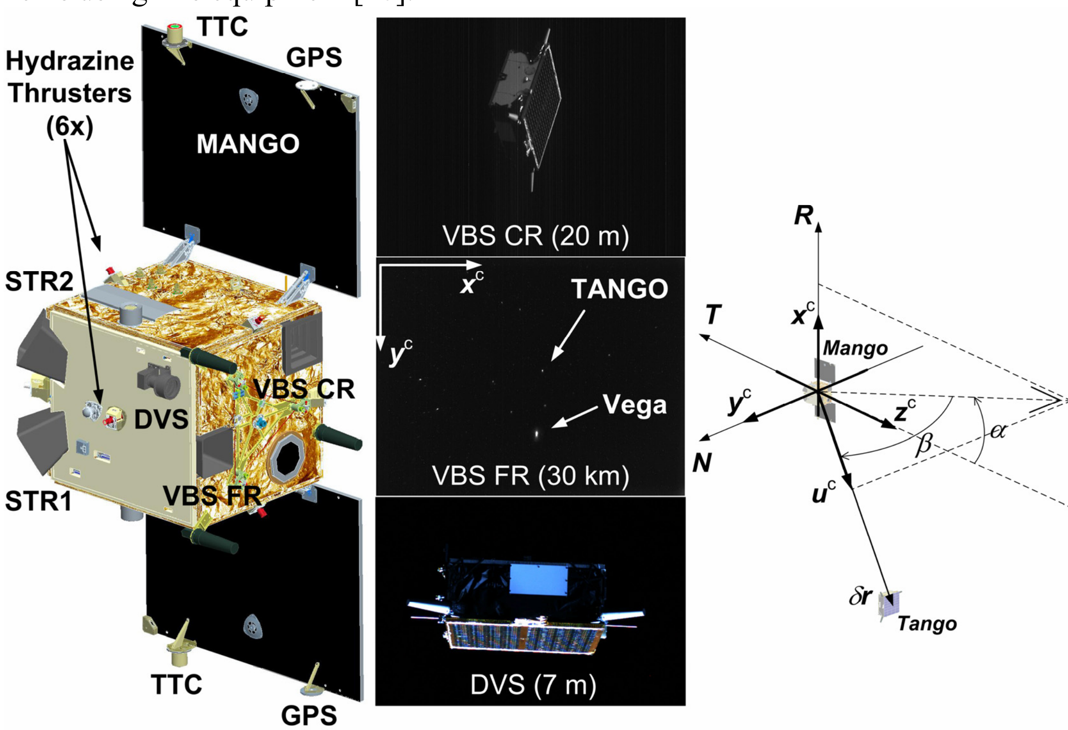

Figure 1. Mango s/c with relevant sensors and actuators (left). Example images of Tango obtained during the mission by the three optical cameras embarked on Mango (middle). Definition of azimuth and elevation angles (α, β) in the far-range camera frame ($x^c y^c z^c$) for a Mango attitude aligned with the orbital frame (RTN).

OHB-Sweden is the prime contractor for the project which is funded by the Swedish National Space Board (SNSB). The German Aerospace Center (DLR), the French National Space Center (CNES) and the Technical University of Denmark (DTU) provide additional support in terms of on-board software and hardware contributions. Among the numerous GNC experiments conducted by the participating organizations, this paper addresses the ARGON in-orbit demonstration of DLR/GSOC.

The VBS optical navigation system embarked on the PRISMA mission and used for this research is based on the microASC platform, a fully autonomous miniature star sensor [7]. VBS hosts four Camera Head Units (CHU) of identical type. These are located at suitable places and directions on the spacecraft, such that a fully redundant blinding free attitude sensor configuration is achieved (see Fig. 1). Two CHUs are used as standard attitude sensors, namely STR1 and STR2. The third CHU, VBS FR, is used as far-range optical sensor and can be pointed in the forward or backward directions (c.f., z^c-axis in Fig. 1), such that the client Tango can be seen in the field of view for most of the mission phases. As compared to the standard star trackers, VBS FR is characterized by an automatic electronic shutter which prevents blinding at intermediate range from Tango. The fourth CHU, VBS CR, is characterized by a modified focal length, iris and electronic shutter, to enable operations at close range with even stronger light conditions. Examples of images taken by the VBS FR, CR, and DVS cameras at different separations during the mission are provided in Fig. 1. DVS is a high resolution color Digital Video System camera which is used for public relation purposes on-board PRISMA.

During ARGON, exclusively VBS FR has been used for angles-only navigation, and only for imaging purposes. The camera can automatically extract so-called regions of interest (ROIs) defined around the brightest objects, typically 2-20 ROIs per image. The ROIs are stored in the mass memory of the servicer on-board computer for later downloads during ground-contacts. As an example, Fig. 1 (middle) shows the first ROIs collected during the experiment on April 23, 2012 at about 30 km separation. Here, Tango is detected for the first time in anti-along-track direction (i.e., $\boldsymbol{z}^c = -\boldsymbol{T}$) based on TLEs, and is seen as a faint dot in the starry sky. Sometimes stars are impressed on the Charge-Coupled Device (CCD) with an apparent luminosity which is higher than the client spacecraft. This is the case for the first image where the star Vega is clearly the brightest visible object.

Table 1. Main parameters of VBS FR camera used during ARGON.

Item	Unit/Type	Value
Position in body frame	m	(-0.090 0.247 0.594)
Orientation in body frame	quaternion	(0.005192706 -0.001818728 0.0008417436 0.9999845)
Half field of view (α_{max},β_{max})	deg	(9.15 6.85)
Camera resolution	pixel	(752 580)
Sun exclusion angle	deg	50
Moon exclusion angle	deg	10
Pixel size	m	$(8.6\ \ 8.3)\cdot 10^{-6}$
Optical axis in CCD plane	pixel	(20 1)
Lens distortion coefficient	ad	$2.6\cdot 10^{-8}$
Effective focal length	m	$20187\cdot 10^{-6}$

For completeness and later usage, a list of key parameters of the VBS FR camera is provided in Table 1. The position of the CCD geometric center is expressed in the Mango body axes. The camera axes are nearly aligned with the spacecraft body axes, and their relative orientation is parameterized through a quaternion. The applied camera model compensates for the radial distortion introduced by lens effects and is described in [7]. In particular, it takes into account the displacement between the CCD geometric center and the optical axis, the non-quadratism effects, and the lens distortion through a correction which is a function of the radial distance in the CCD plane. The field of view, resolution, pixel size, and optical center are provided by Table 1 in camera axes (see Fig. 1). It is noted that half field of view (α_{max} in $\boldsymbol{x}^c$) and pixel size of the VBS FR camera correspond to approximately 4.8 km and 11.6 m at 30 km separation from Tango respectively.

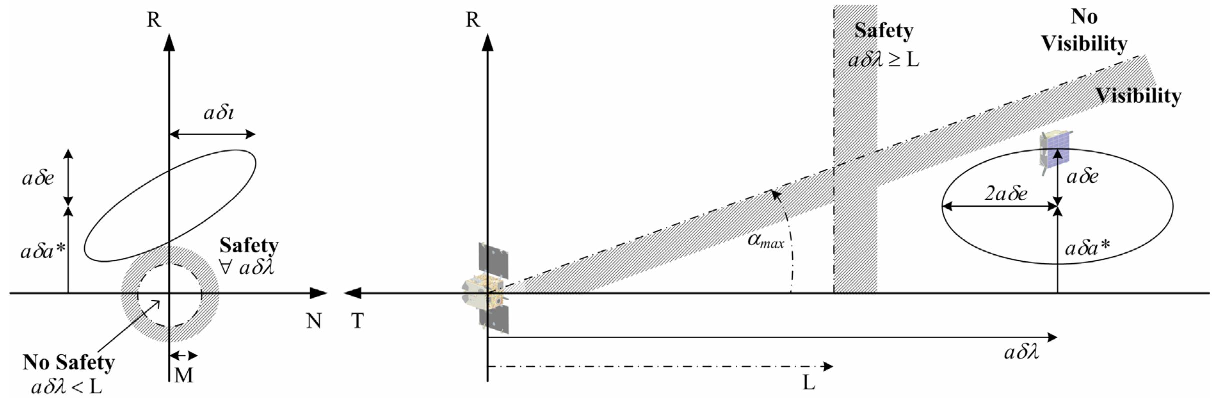

Figure 2. Snapshot of safety and visibility constraints in the Mango RTN orbital frame.

3. Experiment Plan

ARGON has been conceived primarily to demonstrate man-in-the-loop, far-range rendezvous to a non-cooperative, passive, and unknown client using vision-based navigation. The key capabilities which had to be demonstrated by ARGON are i) handover of servicer navigation from NORAD TLEs to optical at large separations, ii) planning/execution of safe unambiguous guidance strategies for far-range rendezvous, iii) collection, analysis, and processing of far-range camera images during rendezvous, iv) routine orbit determination and maneuver calibration of servicer based on GPS raw data, v) routine angles-only relative orbit determination (client w.r.t. servicer), vi) ground-based maneuver planning and execution to track desired guidance profile, and vii) acquisition of no-drift point at a prescribed mean along-track separation from the client.
It is noted that all tasks described above had to rely only on data of the servicer spacecraft available after downlink ground-contacts. Apart from coarse a-priori information available from the NORAD TLE catalogue, the client vehicle is assumed to be unknown and non-cooperative. Furthermore, the specific autonomous navigation functionalities of the VBS system are ignored to extend the generality and portability of ARGON to a servicer spacecraft equipped with standard star trackers only.

3.1. Guidance Profile

The safety and visibility constraints which had to be taken into account in the design of the rendezvous guidance are depicted in Fig. 2. The relative motion of the client vehicle is mapped in the orbital frame centered on the servicer and aligned with the radial (***R***, positive in Zenith direction), along-track (***T***, positive in flight direction), and cross-track (***N***, normal to the orbital plane) directions. The servicer spacecraft body axes can be aligned with the orbital frame in such a way that the VBS FR camera is always oriented in flight ($\boldsymbol{z}^c = \boldsymbol{T}$) or anti-flight ($\boldsymbol{z}^c = -\boldsymbol{T}$) direction. The nominal attitude can be selected on-ground depending on the expected location of the client ahead or behind the servicer respectively. On the contrary, the client spacecraft rotates with an angular velocity of about 0.12 deg/s (i.e., two revolutions per orbit), in order to emulate a slowly tumbling passive objects. The following set of relative orbital elements [11]

$$
\boldsymbol{x} = \begin{pmatrix} \delta a \\ \delta e_x \\ \delta e_y \\ \delta i_x \\ \delta i_y \\ \delta u \end{pmatrix} = \begin{pmatrix} \delta a \\ \delta e \cos\varphi \\ \delta e \sin\varphi \\ \delta i \cos\vartheta \\ \delta i \sin\vartheta \\ \delta u \end{pmatrix} = \begin{pmatrix} (a - a^{\mathrm{o}})/a^{\mathrm{o}} \\ e\cos(\omega) - e^{\mathrm{o}}\cos(\omega^{\mathrm{o}}) \\ e\sin(\omega) - e^{\mathrm{o}}\sin(\omega^{\mathrm{o}}) \\ i - i^{\mathrm{o}} \\ (\Omega - \Omega^{\mathrm{o}})\sin(i^{\mathrm{o}}) \\ (u - u^{\mathrm{o}}) \end{pmatrix} \tag{1}
$$

is adopted to parameterize the relative motion and to express the aforementioned constraints in a convenient way. Here a, e, i, ω, Ω, and M denote the classical Keplerian elements, whereas $e = (e\cos\omega \;\; e\sin\omega)^{t}$, and $u = M + \omega$ represent the eccentricity vector and the mean argument of latitude. The superscript "o" denotes quantities referring to the reference spacecraft which defines the origin of the orbital frame (here the servicer). Under the assumptions of the Hill-Clohessy-Wilshire equations [13], the magnitude of the relative eccentricity and inclination vectors, δe and δi, provide the amplitudes of the in-plane and out-of-plane relative motion oscillations, whereas relative semi-major axis, δa, and relative mean longitude, $\delta\lambda = \delta u + \delta i_{\mathrm{y}}\cot(i^{0})$, provide mean offsets in radial and along-track directions respectively. The orientation of the shape of the relative motion is driven by the phase angles φ and ϑ, which identifies the mean argument of latitude of the perigee and ascending node of the relative orbit [11].

According to Fig. 2, the visibility constraints can be expressed as

$$
\begin{cases} |\delta \mathrm{e} + \delta \mathrm{a}^*| / |\delta\lambda| < \tan(\alpha_{\max}) \\ \delta \mathrm{i} / |\delta\lambda| < \tan(\beta_{\max}) \end{cases} \tag{2}
$$

where the camera axes are assumed to be aligned with the orbital frame (see Fig. 1). Whereas $\delta a^* = \delta a - \delta\lambda^2/2$ has been introduced to take into account the curvature of the orbit at large separations. The safety concept is based on the well known relative eccentricity and inclination vector separation method [11]. In the presence of large uncertainties in the along-track separation, such as with angles-only navigation, the collision risk is measured as a function of the radial and cross-track separations. These can be minimized through a formation configuration with (anti-)parallel $\boldsymbol{\delta e}$ and $\boldsymbol{\delta i}$. In this case, the minimum separation perpendicular to the flight direction, $\delta r_{\mathrm{RNmin}}$, is given by the vector magnitudes and the relative motion can be considered safe if one of following conditions is valid

$$
\begin{cases} \delta r_{\mathrm{RN\,min}} = a^0 \min(\delta i, \delta e - |\delta a^*|) > \mathrm{M} & \text{for} \quad a^0 \delta\lambda < \mathrm{L} \\ \delta r_{\mathrm{RN\,min}} = a^0 \min(\delta i, \delta e - |\delta a^*|) \geq 0 & \text{for} \quad a^0 \delta\lambda \geq \mathrm{L} \end{cases} \tag{3}
$$

Here, M represents a safety threshold for the minimum separation perpendicular to the flight direction, whereas L is an along-track separation which shall be selected large enough to provide inherent safety independently from the formation shape, orientation, and the relative navigation errors. The regions of (non-)visibility and (non-)safety defined by Eqs. (2,3) are depicted in Fig. 2 through dashed areas. It is noted that for short mean along-track separations, the safety constraint is only violated if the minimum between the radial and cross-track separations lies within the indicated no-safety region.

The overall set of aimed relative orbital elements throughout ARGON is referred to as guidance profile. The goal is to first acquire an anti-parallel configuration of $\delta\boldsymbol{e}$ and $\delta\boldsymbol{i}$, and then reduce the magnitude of these vectors in a step-wise manner. In parallel, the relative mean argument of latitude (or mean along-track separation) is reduced through step-wise corrections of the relative semi-major axis. The finally aimed formation configuration corresponds to a delivery geometry with zero along-track drift (or zero relative semi-major axis). On one hand, the relative navigation errors are expected to be larger at experiment start because of the reduced observability (and initial TLE navigation errors). On the other hand, the visibility and safety constraints as well as the control accuracy objectives have more weight at experiment end, close to the delivery time. These aspects drive the selection of a guidance profile characterized by changes of the relative orbital elements which are first gradually increased, and later decreased with maximum corrections at experiment half. The initial and final aimed formation geometries result from a trade-off which takes into account the visibility and safety constraints given by Eqs. (2,3) in the presence of navigation and control uncertainties [14].

In particular the initial nominal formation geometry to be acquired was chosen at 30 km mean along-track separation ($a^{o}\delta\lambda$ = -30 km), with no along-tack drift rate ($a^{o}\delta a$ = 0), and amplitudes of the radial and cross-track oscillations of 400 m ($a^{o}\delta i_{y} = - a^{o}\delta e_{y}$ = 400 m, $a^{o}\delta e_{x} = a^{o}\delta i_{x}$ = 0). The selected relative orbital elements ensure visibility of the client spacecraft in the presence of typical NORAD TLE uncertainties of 500 m in the components of $a\delta\boldsymbol{e}$ and $a\delta\boldsymbol{i}$ [14]. The final aimed formation geometry was selected as $a^{o}\delta i_{y} = - a^{o}\delta e_{y}$ = 150 m and $a^{o}\delta\lambda$ = -3 km. This ensures safety and visibility in the presence of angles-only navigation errors with standard deviations of 3 m ($a^{o}\delta a$), 30 m ($a^{o}\delta e = a^{o}\delta i$), and 300 m ($a^{o}\delta\lambda$) as expected from high-fidelity simulations conducted in preparation of ARGON [12]. The injected maneuver execution errors are of about 1 mm/s with a maneuver cycle of 24 hours, these figures are driven by the ARGON operations concept which is described in the following section.

3.2. Operations Concept

The ARGON experiment operations concept includes three major elements, namely the PRISMA Mission Control Center (MCC), the Experiment Control Center (ECC), both located at Stockholm/Solna, and the ESRANGE/Kiruna ground-station. The MCC is under OHB-SE management and has the responsibilities of overall mission control, bus operations and health monitoring among others. The ECC is under DLR/GSOC management and has the overall experiment responsibility, including the operations of the ARGON flight dynamics system described in the next section. The MCC constitutes the ultimate interface between the spacecraft and the ECC. In addition, it was responsible for the acquisition of the formation initial conditions. These were prescribed by ECC in terms of nominal relative orbital elements and associated errors induced by TLE navigation (see Sect. 3.1).

The ESRANGE/Kiruna ground-station was used during ARGON to establish uplink and downlink communication with the spacecraft. This gave approximately 10 passages per day of about 10 minutes duration each. The typical passage schedule is illustrated in Fig. 3, including the main involved activities. For most of the day, all relevant telemetry (TM) data (e.g., attitude, GPS and VBS FR) which are stored in the servicer mass-memory during one orbital revolution (about 100 min.) can be downloaded at the subsequent ground-contact (see Fig. 3, TM Download). Exception is made between 05:00 and 14:00 UTC each day, where Mango is not visible from Kiruna. In order to guarantee the timely availability of data with no delays, the mass-memory pointer was reset at the first contact of the day (ca. 14:00 UTC) in such a way that the most recent data, covering the last 2-hour arc, were downloaded. This approach resulted to be robust enough for routine operations and provided a total of approximately 7-hour long data gaps each day (i.e., btw. 05:00 and 12:00 UTC).

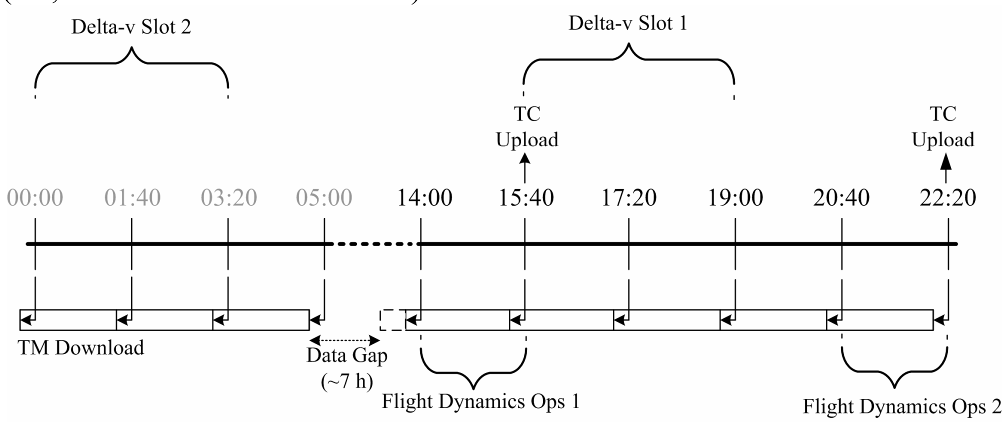

Figure 3. ARGON baseline operational day. The ground-contacts are tagged with the approximate time (UTC) of signal acquisition. Unmanned ground passages are gray.

The core ECC flight dynamics operations were concentrated in two time slots (see Fig. 3, Flight Dynamics Ops 1 and 2) between two subsequent passages over Kiruna. Each operations slot gave the possibility to process the latest income TM through the complete chain of flight dynamics software modules and finally generate the maneuver telecommands (TCs) for upload to the spacecraft by the MCC. In order to minimize the elapsed time between the state estimates performed on-ground (i.e., latest available VBS FR image data) and the maneuver times for formation acquisition/keeping, two delta-v slots have been defined right after and in close vicinity of the planning sessions (see Fig. 3, Delta-v Slot 1 and 2). In addition care was taken to ensure the presence of TM data during maneuver-free periods for at least one orbit before and after the delta-v slots to properly estimate the executed orbit control maneuvers.

4. Flight Dynamics System

In order to fulfill the objectives and constraints introduced in the previous sections a tailored flight dynamics system has been developed for ARGON. A simplified architectural layout of the flight dynamics system is illustrated in Fig. 4. Telemetry data from the servicer is down-linked during ground-contacts, and later processed by the ground-based software. This is used for angles-only relative navigation and subsequent maneuver planning. The resulting Telecommands are sent back to the servicer spacecraft during up-link contacts for the execution of orbit control maneuvers.

After each ground-contact, a sequence of VBS FR ROIs is downloaded from the servicer spacecraft which covers a time frame of approximately one orbital revolution. The available ROIs are assembled in equivalent images which can be processed by the **Image Processing**

(IMP) software at once as a batch. The fundamental task of IMP is to detect a target non-stellar object (here the client Tango satellite) for each given image and convert its measured position into a line-of-sight vector in the camera frame. To this end the camera model described in Table 1 is applied by IMP to account for lens distortion effects. Upon availability of a sufficient number of stars in the field view, the output line-of-sight vector is accompanied by an estimate of the camera inertial attitude which can be used to map it onto the J2000 coordinate system. In its core, IMP consists of five key steps [14]: 1) detection and linking of clusters in the sequence, 2) detection of stars, 3) detection of client, 4) computation of line-of-sight vector, 5) attitude determination.

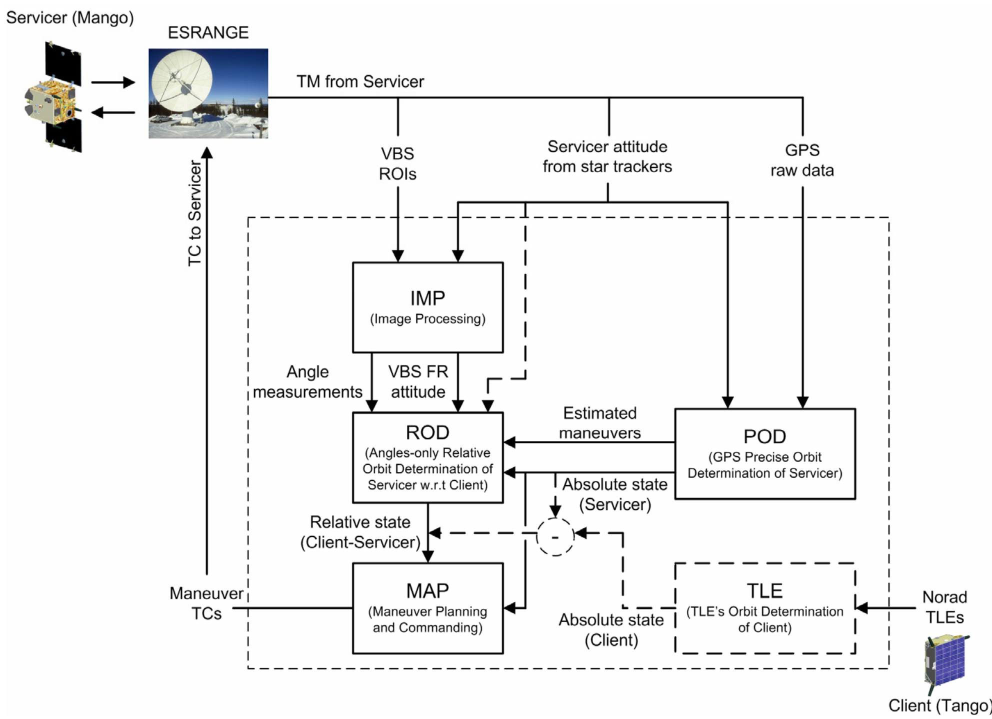

Figure 4. Top-level architecture of flight dynamics system for ARGON.

The line-of-sight vectors $\boldsymbol{u}^c$ (c.f., Fig. 1) provided by IMP are used by the **Relative Orbit Determination (ROD)** module to estimate the relative orbital elements $\boldsymbol{x}$ (c.f., Eq. (1)) at the end time of the measurements arc. This is done through an iterative dynamics batch least-squares estimator with a-priori information. The actual measurements processed by ROD are azimuth, α, and elevation, β, angles which subtend $\boldsymbol{u}^c$, as defined in Fig. 1. In view of a possible implementation in real-time, instead of a rigorous numerical integration of the equations of motion, here a simple relative dynamics model is adopted for the state transition matrix which captures Earth oblateness J_2 effects in near-circular orbits [11]. The variations of the relative orbital elements caused by impulsive maneuvers are modeled under the same assumptions through the inversion of the solution of the Hill-Clohessy-Wiltshire equations. The partial derivatives of the angle measurements w.r.t. relative orbital elements about the reference state are computed making use of the fact that they do not depend on the relative velocity [12,14]. By default the absolute attitude of the VBS FR camera is estimated by IMP based on the stars of the same image. If less than five stars are visible, ROD combines the inertial attitude of the servicer from the standard star trackers with the a-priori knowledge of the camera orientation in body frame (see Table 1). These two modes of operations are also referred to as *astrometry* and *local* modes respectively. Obviously the computation of the state transition and sensitivity matrices requires knowledge of the servicer absolute orbit and its executed orbit control maneuvers. This information is produced by a **Precise Orbit Determination (POD)** process based on single-frequency GPS raw data of the servicer [4]. In the case of a failure of the POD, or as backup, coarse orbit (GPS receiver navigation solutions) and delta-v maneuvers (a-priori info) of the servicer can also be directly retrieved from the TM and used by ROD.

The latest available estimate of the relative state generated by ROD is used by the **Maneuver Planning and Commanding (MAP)** module to compute orbit control maneuvers of the servicer in order to track a pre-defined guidance profile w.r.t. the client. ROD and MAP implements the same relative dynamics model for state propagation. In order to improve the system observability, in-plane and out-of-plane maneuvers are regularly planned and executed at various locations along the orbit. MAP computes the desired orbit corrections as a function of the difference between the desired (guidance) and estimated (from ROD) relative orbit. The necessary delta-v orientation, size and location are computed according to closed-form solutions of the simplified Gauss variational equations [11]. The ultimate output of MAP consists of time-tagged maneuver commands which can be directly sent to the servicer spacecraft during up-link contacts. Prior to the activation of the VBS system, or in general in the absence of VBS FR measurements, a coarse relative orbit is estimated making use of NORAD TLEs for the client and GPS measurements for the servicer. A dedicated **TLE-based orbit determination (TLE)** batch least-squares software module is used to further filter TLEs available from consecutive days prior to the experiment start. It is noted that the initial conditions of the ARGON experiment were acquired by MCC (OHB-SE) introducing the typical control errors induced by TLE-only navigation. In an attempt to mimic a representative lost-in-space scenario, the actual initial relative position and velocity of Mango w.r.t. Tango (derived from GPS data) was not known by DLR/GSOC during the complete experiment.

5. Flight Results

The ARGON flight experiment started on April 23, 2012 - 14:21 UTC (i.e., 650 days from the PRISMA launch). After the first contact, the freshly received servicer GPS and attitude data and the daily NORAD TLEs of the client have been used to determine a coarse estimate of the relative orbit of Tango w.r.t. Mango. The formation geometry was found to be several hundreds of meters off the nominal values in the relative eccentricity and inclination vectors, with a Mango mean along-track separation of 30 km ahead of Tango and a residual drift of ca. 25 m/orbit in anti-velocity direction.

Within one hour after the first contact, the ECC was able to execute the planned sequence of orbit determination and maneuver planning tasks (i.e., modules POD, TLE, and MAP in Fig. 4) and deliver to MCC the desired maneuver commands for upload during the second passage at 16:00 UTC. This passage gave also the possibility to download the first orbit of VBS FR ROIs (see Fig. 1). The handover from NORAD TLEs to vision-based navigation was smoothly performed within the successive three orbits, once a sufficient number of camera measurements was available for angles-only relative orbit determination around the executed orbit control maneuvers (i.e., module ROD in Figure 4). The ARGON flight dynamics system made use of ROI image portions every ca. 30 s. As foreseen by the operational concept two flight dynamics sessions were performed each day. These resulted in the execution of sequences of in-plane and out-of-plane maneuvers in the afternoon and early morning (see Fig. 3) to perform the desired rendezvous and, at the same time, improve the accuracy of the range estimate.

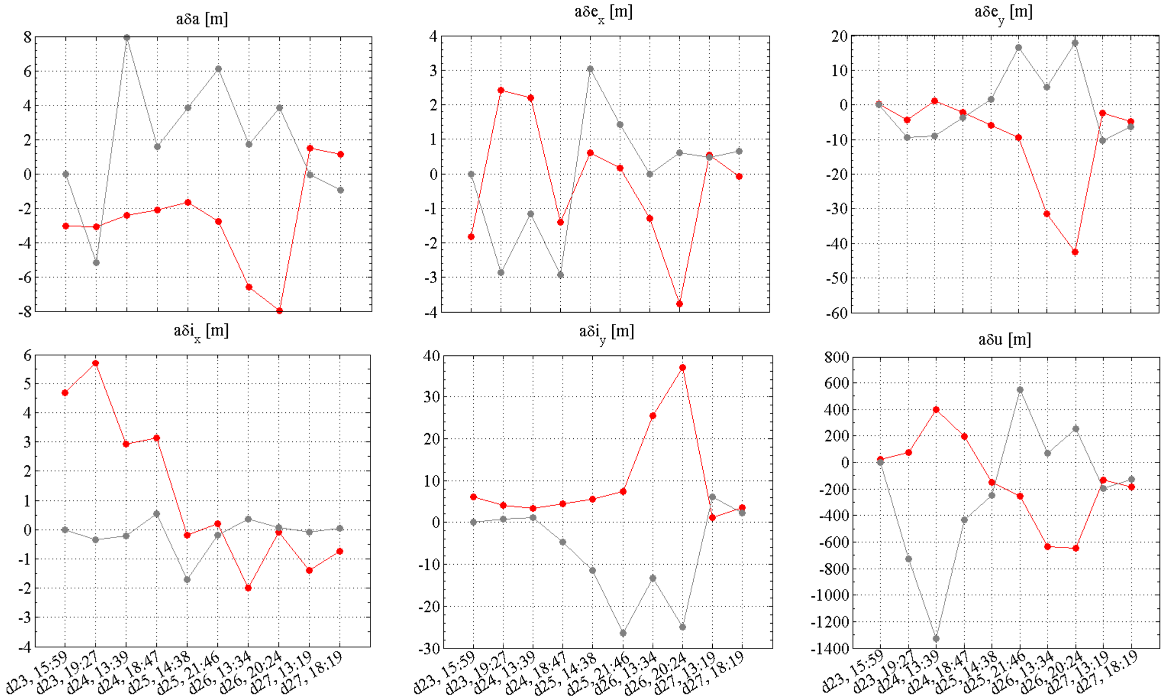

Figure 5. Angles-only ROD errors evaluated at the end of each measurement batch as obtained from comparison with POD flight data (red) and rehearsal simulation (gray).

A comparison of the ROD state estimates obtained during the experiment with the GPS POD products has been done after the conclusion of ARGON as illustrated in Fig. 5 [14]. Here the difference between estimated and reference states is computed at the end time of each measurement batch processed by ROD (red line). Since this state is used by MAP for maneuver planning, its accuracy drives the formation acquisition and keeping performance. The results demonstrate navigation errors which are similar to the ones obtained by the rehearsal tests conducted during the preparation activities (gray line) [12]. For most of the ROD runs, the maximum absolute errors of the estimated relative orbital elements are 3 m in the relative semi-major axis, 10 m in the magnitude of the relative eccentricity/inclination vectors, and 400 m in the mean along-track separation (i.e., about 1% of the initial along-track separation). The overall trend of the relative navigation accuracy indicates a nearly constant behavior with some slight improvements for smaller separations, especially in δa, δe_x and δi_x.

On the contrary, the ROD sessions on April 26, 2012 (i.e., runs 7 and 8 in Fig. 5) are affected by 2-3 times larger errors as compared to the other runs. During this phase, Mango was at separations below 10 km from the client spacecraft. Due to the predefined shutter control settings which regulate the VBS FR image integration time, the stars were badly underexposed in the images which therefore contained only an overexposed cluster associated to Tango. The unavailability of inertial attitude estimates in ROD *astrometry* mode (see Sect. 4) caused a drastic reduction of angle measurements. Only after, the mode of operations of the software was changed to *local* and, despite the larger bias and noise of the measurement residuals (see Fig. 7), the resulting relative navigation accuracy was shown to be comparable with the previous runs (see ROD runs 9 and 10 in Fig. 5). The achieved navigation accuracy allowed a smooth rendezvous from 30 km to the final hold point at 3 km mean separation selected before the start of the experiment. Figure 6 illustrates the resulting relative motion of servicer w.r.t. client as estimated by the GPS POD after the execution of ARGON (red line). Again, the results of the rehearsal simulation (gray line) are shown to be representative of the actual behavior in orbit. The major discrepancy is given by the initial conditions which were affected by different TLE navigation errors.

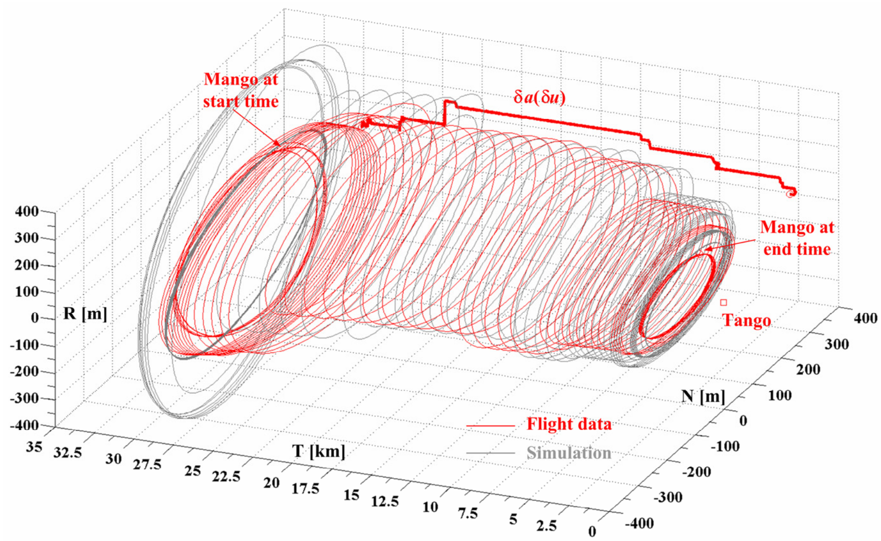

Figure 6. Relative position of Mango w.r.t Tango (origin) as from POD flight data (red) and rehearsal simulation (gray).

A fundamental functionality of the IMP module is the client centroiding algorithm. The centroiding performance has been assessed by comparing the measured client 2D position coordinates in the CCD frame with the true value derived by GPS POD. The reference relative position of Mango w.r.t. Tango is converted from the inertial frame to the camera frame through the usage of the camera model of Table 1 [7]. The computed errors and their statistics are illustrated in Fig. 7 (red) and cover the complete ARGON experiment duration. The rehearsal simulation results are superimposed in gray color. The best centroiding performance has been achieved at the beginning of the experiment with large inter-spacecraft separations. Here the systematic errors are shown to be about 20% of the pixel size (i.e., ~16 arcsecs), whereas the standard deviation of the noise error is about 50% of the pixel size (i.e., ~40 arcsecs).

First of all, the centroiding error is not uniformly distributed but rather exhibits a once-per-revolution pattern. This phenomenon does not affect star centroids and is due to the fact that the light reflected by the imaged target depends on the illumination conditions in combination with its rotating attitude. Secondly, a dramatic degradation of performance is observed in the $\boldsymbol{y}^c$ camera axis during the last days of the experiment (see Fig. 7 - bottom). This is due to the decreasing separation which induces an enlargement of the object size as pictured in the camera images. An interesting anomaly is observed when looking directly at ROIs provided by the camera. Fig. 7 (right) shows two examples from April 26, 2012. Here a truncation of the cluster associated to the client object is clearly visible, which in turn results in centroiding errors up to several pixels. The measured pixel coordinates are represented by a circle, whereas the object center retrieved via GPS POD is represented by a star in Fig. 7. This error seems to be dependent on the client attitude, but also on the ability of the camera to center properly the region of interest. The provided samples demonstrate that, within a limited time period (here nearly one orbit), the centroiding performance can change from a nominal to a degraded status because of truncation effects. An attempt was made to introduce this phenomenon in the rehearsal simulations through jumps of 0.5 to 1 pixel in the mean error of the azimuth and elevation angles (see discontinuities in gray line of Fig. 7).

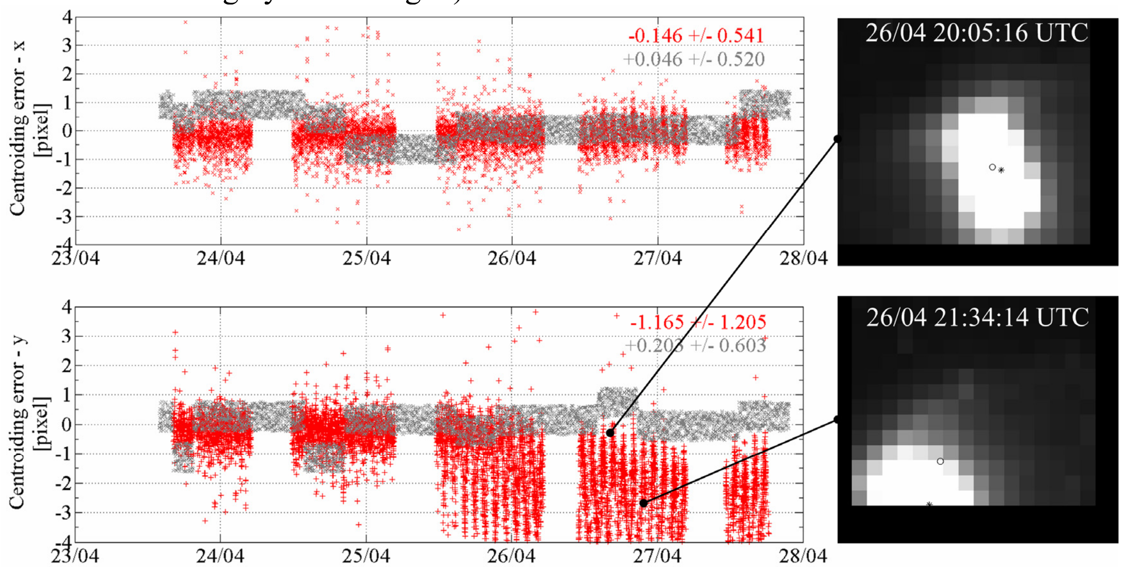

Figure 7. IMP centroiding errors (left) and truncation effects (right) as obtained from comparison with POD flight results (red) and rehearsal simulation (gray).

Regarding the MAP in-orbit results, the relative eccentricity and inclination vectors have been properly aligned in a safe anti-parallel configuration in a step-wise manner throughout the experiment. The magnitude of the radial and cross-track oscillations has been decreased from ca. 300-400 m to 150 m at the end configuration to always keep Tango in the camera field of view and, at the same time, guarantee a minimum separation perpendicular to the flight direction at all times. After recovery of the initial dispersion due to TLE-navigation, the relative semi-major axis has been gradually decreased to ca. -140 m (see Fig. 6 – δa) to establish the maximum drift (ca. -1.5 km/orbit) on April 25, 2012, and progressively increased to its final value around -0.4 m at the end of ARGON on April-27, 2012 - 21:40 UTC. The mean along-track separation was affected by a control error of about 300 m throughout the rendezvous, i.e. 1% of the initial separation. The amplitude of the relative eccentricity and inclination vectors deviated by less than 20 m (rms) from the desired values. It is noted that the rendezvous performance has been slightly degraded by the decrease of navigation accuracy on April 26. The overestimation of the relative semi-major axis induced a temporary drift of Mango w.r.t. Tango in along-track direction (i.e., opposite to nominal) and small undesired changes of the relative eccentricity and inclination vectors. These caused minimum separations perpendicular to the flight direction of 110 m on the morning of April 27. The control accuracy got back to normal values in the afternoon, after the first maneuver planning session of the day. This allowed the acquisition of the aimed final formation geometry within the expected error margins at the end of the experiment. The total delta-v consumed during ARGON has been approximately 1 m/s, i.e., half of the originally allocated budget.

6. Lessons Learned and Conclusions

This paper has presented system design and flight results from ARGON, one the first demonstrations of non-cooperative far-range rendezvous in low Earth orbit based on angles-only measurements. For the first time, specifically developed techniques and software modules have been exercised during actual mission operations in a ground-in-the-loop fashion. The technology presented in this paper could demonstrate reliable, safe and accurate far-range approach to a passively rotating vehicle using angles-only measurements for navigation and relative eccentricity/inclination vectors for guidance and control. In addition, the post-facto availability of independent and accurate navigation information coming from relative GPS gave the possibility to properly evaluate the achieved navigation and control accuracies.

Four relevant items need to be mentioned here for future assessment. First of all the accuracy of the angles-only relative navigation is strictly dependent on the adopted camera hardware, its resolution, and an appropriate bias calibration. In the PRISMA case, the VBS far-range camera has a pixel size of ca. 80 arcsecs. This drives the noise of the line-of-sight measurements which has been found to be 50% of the pixel size during ARGON (~40 arcsecs). A simple star tracker camera calibration model has been adopted to take into account effects such as lens distortion, non-quadratism and offsets between optical and geometric axes which accounts for measurement biases up to 1-2 pixels. As a result, residual systematic offsets of the order of 16 arcsecs (~20% of pixel size) have been achieved at large separations (> 10 km). In order to further improve the quality of the measurements, an effort should be put into the improvement of the centroiding function and its integration within an on-line calibration process.

Second, due to the limitations encountered with the servicer telemetry data-rate budget, only so-called regions of interest (ROIs) extracted from raw camera images could be downloaded and used for navigation during ARGON. On one hand, this simplifies the image processing performed on ground which is asked to process only 10-15 ROIs per image. On the other hand, the generated ROIs have a limited size and are often subject to overflow effects where a substantial area of the light cluster associated to the client is cutoff. This phenomenon causes undesirable biases in the extracted measurements, especially at close separations, which are difficult if not impossible to estimate.

Third, the illumination conditions of the ARGON experiment have to be considered. The observed once-per-revolution pattern of the angle measurement residuals suggests that the attitude motion of the client affects significantly the shape of the light cluster as pictured by the camera. Furthermore the automatic shutter control of the camera induces illumination of camera pixels in the neighborhood of the target whose shape appears about ten times bigger than theoretically expected. This makes the estimation of the range to target based on apparent diameter measurements, as suggested by various authors, totally unreliable.

Last but not least, the achievable relative navigation accuracy is affected by the adopted processing scheme and by issues of observability. Given the aforementioned camera measurements, relative navigation errors below 5-10 m could be demonstrated throughout the complete rendezvous (i.e., from 30 km down to 3 km separation) on all relative orbital elements, excluded the relative mean argument of latitude. Despite the execution of regular and diverse orbit control maneuvers to obtain an unambiguous set of measurements, the mean along-track separation remained affected by errors substantially larger than what achievable through radar or lidar tracking. This intrinsic limitation of angles-only relative navigation calls for a deeper analysis of the guidance profile which should be specifically optimized for navigation accuracy.

Despite the aforementioned limitations, this work has not only shown the viability of angles-only navigation for long-term rendezvous operations, but also its high technology readiness level through its simplicity and robustness. The technology developed during ARGON will find relevant applications in present and future missions which foresee DLR/GSOC involvement. Ultimately the intention is to transfer the ARGON technology to a servicer spacecraft in order to perform fully autonomous vision-based rendezvous to a non-cooperative target.

7. References

[1] Weismuller, T., and Leinz, M., "GN&C Technology Demonstrated by the Orbital Express Autonomous Rendezvous and Capture Sensor System," AAS Paper 06-016, 2006.

[2] Rupp, T., Boge, T., Kiehling, R., Sellmaier, F., "Flight Dynamics Challenges of the German On-Orbit Servicing Mission DEOS," 21st International Symposium on Space Flight Dynamics (ISSFD), 28 Sep. - 2 Oct. 2009, Toulouse, France, 2009.

[3] Ardaens, J.-S., D'Amico, S., Fischer, D., "Early Flight Results from the TanDEM-X Autonomous Formation Flying System," 4th International Conference on Spacecraft Formation Flying Missions & Technologies (SFFMT), 18-20 May 2011, St-Hubert, Quebec, 2011.

[4] D'Amico, S., Ardaens, J.-S., Larsson, R., "Spaceborne Autonomous Formation-Flying Experiment on the PRISMA Mission," Journal of Guidance, Control, and Dynamics 2012, 0731-5090, vol.35 no. 3 (834-850), May-June 2012, doi: 10.2514/1.55638.

[5] Woffinden, D.C., and Geller, D.K., "Navigating the Road to Autonomous Orbital Rendezvous," Journal of Spacecraft and Rockets 2007, vol. 44, no. 4 (898-909), July–August 2007, doi: 10.2514/1.30734.

[6] Chari, R. J. V., "Autonomous Orbital Rendezvous Using Angles-Only Navigation," Master's thesis, Massachusetts Institute of Technology, June 2001.

[7] Benn, M., "Vision Based Navigation Sensors for Spacecraft Rendezvous and Docking", PhD thesis, DTU, October 2010.

[8] Woffinden, D.C., "On Orbit Satellite Inspection," Master's thesis, MIT, Cambridge, MA, 2004.

[9] Schmidt, J., Geller, D.K., Chavez, F., "Viability of Angles-only Navigation for Orbital Rendezvous Operation," AIAA 2010-7755, AIAA Guidance, Navigation, and Control Conference, 2-5 August 2010, Toronto, Ontario Canada, 2010.

[10] Bodin, P., Noteborn, R., Larsson, R., Karlsson, T., D'Amico, S., Ardaens, J.-S., Delpech, M., Berges, J.-C., "Prisma Formation Flying Demonstrator: Overview and Conclusions from the Nominal Mission," AAS 12-072; 35th Annual AAS Guidance and Control Conference, 3-8 Feb. 2012, Breckenridge, Colorado (2012).

[11] D'Amico, S., "Autonomous Formation Flying in Low Earth Orbit," PhD thesis, TU Delft, March 2010.

[12] Gaias, G., D'Amico, S., Ardaens, J.-S., "Angles-only Navigation to a Non-Cooperative Satellite using Relative Orbital Elements," AIAA/AAS Astrodynamics Specialists Conference, Minneapolis, MN, 13-16 August 2012.

[13] Clohessy, W. H., and Wiltshire, R. S., "Terminal Guidance System for Satellite Rendezvous," Journal of the Aerospace Sciences, Vol. 27, 1960, pp. 653–658.

[14] D'Amico, S., Ardaens, J.-S., Gaias, G., Benninghoff, H., Schlepp, B., Jørgensen, J.L., "Non-Cooperative Rendezvous using Angles-only Optical Navigation: System Design and Flight Results," Submitted to Journal of Guidance, Control, and Dynamics (2012).